The Journal of Immunology

RESEARCH ARTICLE | APRIL 01 2005

Molecular Circuits of Resolution: Formation and Actions of Resolvins and Protectins[1]

Gerard L. Bannenberg; ... et. al

J Immunol (2005) 174 (7): 4345–4355.
https://doi.org/10.4049/jimmunol.174.7.4345

Molecular Circuits of Resolution: Formation and Actions of Resolvins and Protectins[1]

Gerard L. Bannenberg,[2] Nan Chiang,[2] Amiram Ariel, Makoto Arita, Eric Tjonahen, Katherine H. Gotlinger, Song Hong, and Charles N. Serhan[3]

The cellular events underlying the resolution of acute inflammation are not known in molecular terms. To identify anti-inflammatory and proresolving circuits, we investigated the temporal and differential changes in self-resolving murine exudates using mass spectrometry-based proteomics and lipidomics. Key resolution components were defined as resolution indices including Ψ_{max}, the maximal neutrophil numbers that are present during the inflammatory response; T_{max}, the time when Ψ_{max} occurs; and the resolution interval (R_i) from T_{max} to T_{50} when neutrophil numbers reach half Ψ_{max}. The onset of resolution was at ~12 h with proteomic analysis showing both haptoglobin and S100A9 levels were maximal and other exudate proteins were dynamically regulated. Eicosanoids and polyunsaturated fatty acids first appeared within 4 h. Interestingly, the docosahexaenoic acid-derived anti-inflammatory lipid mediator 10,17*S*-docosatriene was generated during the R_i. Administration of aspirin-triggered lipoxin A_4 analog, resolvin E1, or 10,17*S*-docosatriene each either activated and/or accelerated resolution. For example, aspirin-triggered lipoxin A_4 analog reduced Ψ_{max}, resolvin E1 decreased both Ψ_{max} and T_{max}, whereas 10,17*S*-docosatriene reduced Ψ_{max}, T_{max}, and shortened R_i. Also, aspirin-triggered lipoxin A_4 analog markedly inhibited proinflammatory cytokines and chemokines at 4 h (20–50% inhibition), whereas resolvin E1 and 10,17*S*-docosatriene's inhibitory actions were maximal at 12 h (30–80% inhibition). Moreover, aspirin-triggered lipoxin A_4 analog evoked release of the antiphlogistic cytokine TGF-β. These results characterize the first molecular resolution circuits and their major components activated by specific novel lipid mediators (i.e., resolvin E1 and 10,17*S*-docosatriene) to promote resolution. ***The Journal of Immunology,*** **2005, 174: 4345–4355.**

Resolution of inflammation is required for the return from inflammatory disease to health, i.e., catabasis (1). It is currently held that many inflammatory diseases are often the result of excessive inflammatory responses, or recurrent and chronic periods of inflammation that fail to resolve (2). Inflammation is now recognized as a central causative event for several of the most common human diseases in the developed world, such as atherosclerosis, cancer, asthma, autoimmune disease, caries, and various neuropathological disorders such as stroke, Alzheimer's, and Parkinson diseases (3, 4). Thus, inflammation has been studied in detail at the molecular, cellular, and pathobiological level, and a great number of factors have been identified that can initiate, modulate, and inhibit acute inflammation (3–6). New evidence from this laboratory indicates that the catabasis from inflammation to the "normal" noninflamed state is not merely the passive termination of inflammation but rather an actively regulated program of resolution (7). Hence, identification of the major cellular events and molecular signals that determine the end of inflammation and the beginning of resolution is a clear requirement for defining resolution (5, 8–11) and could provide the molecular basis for treatment and prevention of inflammatory diseases.

A body of new evidence demonstrates that endogenous mediators actively participate in dampening host responses to orchestrate resolution. For example, 5*S*,6*R*,15*S*-trihydroxy-7,9,13-*trans*-11-*cis*-eicosatetraenoic acid (LXA_4)[4] is generated from arachidonic acid (AA) via lipoxygenase pathways during cell-cell interactions. In addition, aspirin acetylates cyclooxygenase-2 and triggers the formation of a LXA_4 epimer, namely aspirin-triggered 15-epi-LXA_4 (ATL) (12). LXA_4 and ATL are the first autacoids recognized as endogenous anti-inflammatory lipid mediators relevant in resolution via activation of a specific G protein-coupled receptor, namely LXA_4 receptor (13, 14). Together, they down-regulate or "stop" polymorphonuclear neutrophil (PMN) infiltration in vitro and in vivo, and thus appear to function as "braking signals" during the time course of inflammation (reviewed in Refs. 8 and 15). Along these lines, recent studies in our laboratory identified novel arrays of lipoxygenase- and cyclooxygenase-2-derived mediators generated from dietary polyunsaturated fatty acids (PUFA), i.e., eicosapentaenoic acid (EPA) and docosahexaenoic acid (DHA). These novel di- and trihydroxy-containing omega-3 PUFA-derived lipid autacoids, termed resolvins, docosatrienes, and neuroprotectins, display potent anti-inflammatory and proresolving actions (9, 16, 17). Given the notion that these mediators are generated endogenously during defined intervals within the acute inflammatory response (9), the view emerges that they may not necessarily serve

Center for Experimental Therapeutics and Reperfusion Injury, Department of Anesthesiology, Perioperative and Pain Medicine, Brigham and Women's Hospital and Harvard Medical School, Boston, MA 02115

Received for publication July 20, 2004. Accepted for publication January 18, 2005.

The costs of publication of this article were defrayed in part by the payment of page charges. This article must therefore be hereby marked *advertisement* in accordance with 18 U.S.C. Section 1734 solely to indicate this fact.

[1] G.L.B. is the recipient of a Postdoctoral Fellowship from the Arthritis Foundation, and A.A. is the 2003 recipient of the McDuffie Postdoctoral Fellowship Award from the Arthritis Foundation. This work was supported in part by National Institutes of Health Grants GM 38765, PO-1-DE 13499, and P50-DE016191 (to C.N.S.).

[2] G.L.B. and N.C. contributed equally to this paper.

[3] Address correspondence and reprint requests to Dr. Charles N. Serhan, Center for Experimental Therapeutics and Reperfusion Injury, Department of Anesthesiology, Perioperative and Pain Medicine, Brigham and Women's Hospital, Boston, MA 02115. E-mail address: cnserhan@zeus.bwh.harvard.edu

[4] Abbreviations used in this paper: LXA_4, lipoxin A_4 (5*S*,6*R*,15*S*-trihydroxy-7,9,13-*trans*-11-*cis*-eicosatetraenoic acid); AA, arachidonic acid; ATL, aspirin-triggered 15-epi-LXA_4; DHA, docosahexaenoic acid; EPA, eicosapentaenoic acid; LC-MS-MS, liquid chromatography-tandem mass spectrometry; LTB_4, leukotriene B_4; PUFA, polyunsaturated fatty acid; R_i, resolution interval; RvE1, resolvin E1; 2D, two-dimensional; 17*S*-HDHA, 17*S*-hydroxy-docosahexaenoic acid; PMN, polymorphonuclear neutrophil; pI, isoelectric point.

0022-1767/05/$02.00

solely to block and/or inhibit inflammation, but may also activate resolution within the inflammatory exudate and thus promote the return to homeostasis (i.e., catabasis as used here is defined as pertaining to the decline of a disease state) (14).

In the present report, we determined the cellular composition during inflammation-resolution using a widely studied murine peritonitis model (18, 19) and first define resolution in operative and quantitative terms to qualify unbiased parameters, namely, the resolution indices. In addition, using the side-by-side lipidomic- and proteomic-based approach (Fig. 1), we obtained the first temporal profile of the major cellular and molecular components involved in resolution. Moreover, administration of the novel PUFA-derived lipid mediators (e.g., resolvins and protectins) differentially regulated these indices.

Materials and Methods

Murine peritonitis

Male FVB mice (6–8 wk; Charles River Laboratories) were anesthetized with isoflurane. ATL analog (ATLa), resolvin E1 (RvE1), 10,17*S*-docosatriene (10,17*S*-DT), or vehicle alone were administered i.p. in 200 μl of sterile saline, 5 min before i.p. administration of 1 mg of zymosan A. At indicated time points, mice were euthanized with an overdose of isoflurane, and peritoneal exudates were collected by lavaging with 5 ml of sterile saline. Exudate cells and supernatants were obtained by centrifugation for analyses described below (also see Fig. 1).

Differential leukocyte counts and FACS analysis

Aliquots of lavage cells were prepared for determination of total and differential leukocyte counts as in Refs. 7 and 20). For determination of cellular composition (PMN vs mononuclear cells), cells were blocked with anti-mouse CD16/32 blocking Ab (0.5 μg/0.5 $\times$ 10^6 cells) for 5 min and stained (20 min) with FITC-conjugated anti-mouse CD14 and PE-conjugated anti-mouse Ly-6G (0.5 μg/0.5 $\times$ 10^6 cells; clones rmC5-3 and RB6-8C5, respectively from BD Pharmingen). For determining macrophage population(s), cells were blocked with anti-mouse CD16/32 blocking Ab (0.5 μg/0.5 $\times$ 10^6 cells) for 5 min and stained (20 min) with FITC-conjugated anti-mouse F4/80 (0.5 μg/0.5 $\times$ 10^6 cells; eBioscience) and PerCP-Cy5.5-conjugated anti-mouse CD11b (0.5 μg/0.5 $\times$ 10^6 cells; BD Pharmingen). Cells were then washed and analyzed by FACSort (21).

Proteomics

Two-dimensional (2D) gel electrophoresis. Supernatants from peritoneal lavages were collected by centrifugation (15 min, 1800 rpm) in the presence of protease inhibitors (Roche). Protein concentration was determined by the method of Lowry (22) (BioRad DC Assay; Bio-Rad). The bulk of albumin was removed using Montage Albumin Deplete spin columns (Millipore) according to manufacturer's instructions. Albumin-depleted protein was concentrated by chloroform/methanol precipitation (23). Exudate proteins were then separated by isoelectric focusing for 45,000 V/h on linear 11-cm (pH 3–10) IPG strips (Bio-Rad) (24). The focused proteins were reduced with DTT, alkylated with iodoacetamide, and fractionated by SDS-PAGE (range ~14–200 kDa). Gels were stained with Sypro Ruby (25), visualized by fluorescence (λ_{ex} 532 nm), and digital images were taken for image analysis (Melanie 4.03; GeneBio). Temporal profiles of particular proteins were obtained by calculating the average intensity of corresponding spots from three to six separate gels by using the class report tool provided by the software.

Liquid chromatography-tandem mass spectrometry (LC-MS-MS) analysis. Protein spots of interest were excised and in-gel digested with trypsin (26). Tryptic peptides were loaded onto a 2-μg capacity peptide trap (CapTrap; Michrom Bioresources) in 2% acetonitrile, 0.1% formic acid, and 0.005% trifluoroacetic acid, and separated by capillary liquid chromatography using a capillary column (75 μm $\times$ 15 cm $\times$ 3 μm; LC Packings) at 150 nl/min delivered by an Agilent 1100LC pump (400 μl/min) and a flow splitter (Accurate; LC Packings). A mobile phase gradient was run using mobile phase A (2% acetonitrile/0.1% formic acid) and B (80% acetonitrile/0.1% formic acid), from 0 to 10 min with 0–20% B followed by 10–90 min with 20–60% B. Peptide mass and charge was determined on a ThermoFinnigan Advantage ion-trap mass spectrometer after electrospray ionization using end-coated spray tips (Silicatip 5 cm, ID 360 μm, tip ID 15 μm; New Objective) held at a spray voltage of 1.8 kV (27, 28). After acquisition of the peptide parent ion mass, zoom scans and tandem mass spectra of parent peptide ions above a signal threshold of 2 $\times$ 10^4 were recorded with dynamic exclusion, using Xcalibur 1.3 data acquisition software (ThermoFinnigan).

Proteins were identified by peptide mapping of tryptic peptide tandem mass spectra using TurboSequest (BioWorks 3.1 software; ThermoFinnigan) (29), using the National Center for Biotechnology Information nr.fasta protein database indexed for mouse proteins. Protein modifications that were taken into consideration included methionine oxidation and alkylation of cysteine with iodoacetamide or acrylamide. A protein was considered identified when a minimum of two tryptic peptides were matched, with a cross-correlation score above 2.0 for at least one peptide.

Mediator lipidomics (LC-UV-MS-MS)

Aliquots of supernatants were extracted with deuterium-labeled internal standards (30 ng of deuterium-labeled PGE_2 and 50 ng of deuterium-labeled AA (Cayman Chemical)) using C18 solid phase extraction (Alltech

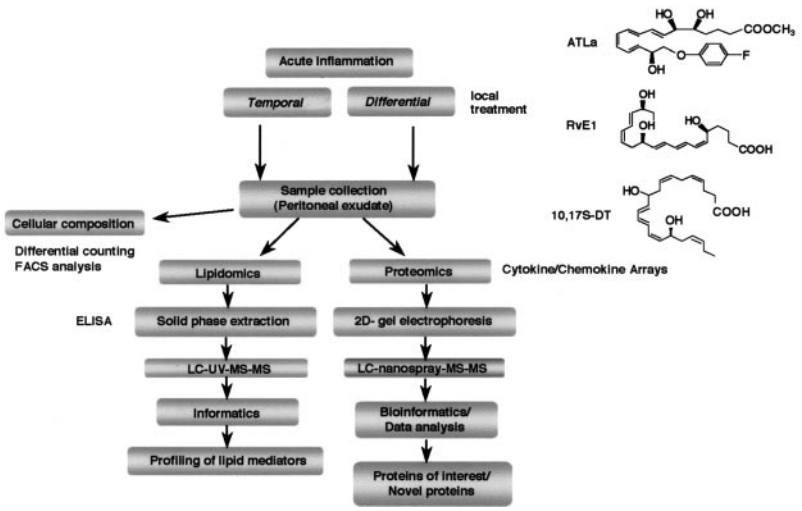

FIGURE 1. Temporal-differential lipid mediator and proteomic analyses of resolution. Zymosan-initiated murine peritonitis (1 mg of zymosan A injected i.p.) was used as a model for acute inflammation. For temporal analysis, peritoneal exudates were collected by lavage at 0, 2, 4, 12, 24, 48, and 72 h. The cellular composition was determined by FACS analysis and differential leukocyte counting with light microscopy. The supernatants were collected for lipidomic and proteomic analyses, and total exudate protein quantitated. Lipidomic analysis was conducted to determine eicosanoids and DHA-derived lipid mediators as well as the precursor fatty acids (i.e., AA, EPA, and DHA) using LC-UV-MS-MS analysis or ELISA. Proteomic analysis was conducted to analyze the composition of exudate proteins using 2D-gel electrophoresis, image analysis, and LC-MS-MS-based identification of individual proteins. Cytokines and chemokines were quantitated by multiplex sandwich ELISA. For differential analysis, zymosan A was administrated alone or with lipid mediators, namely ATLa, RvE1, or 10,17*S*-docosatriene 10,17*S*-DT; (300 ng each injected i.p.) and the analyses were conducted as described above.

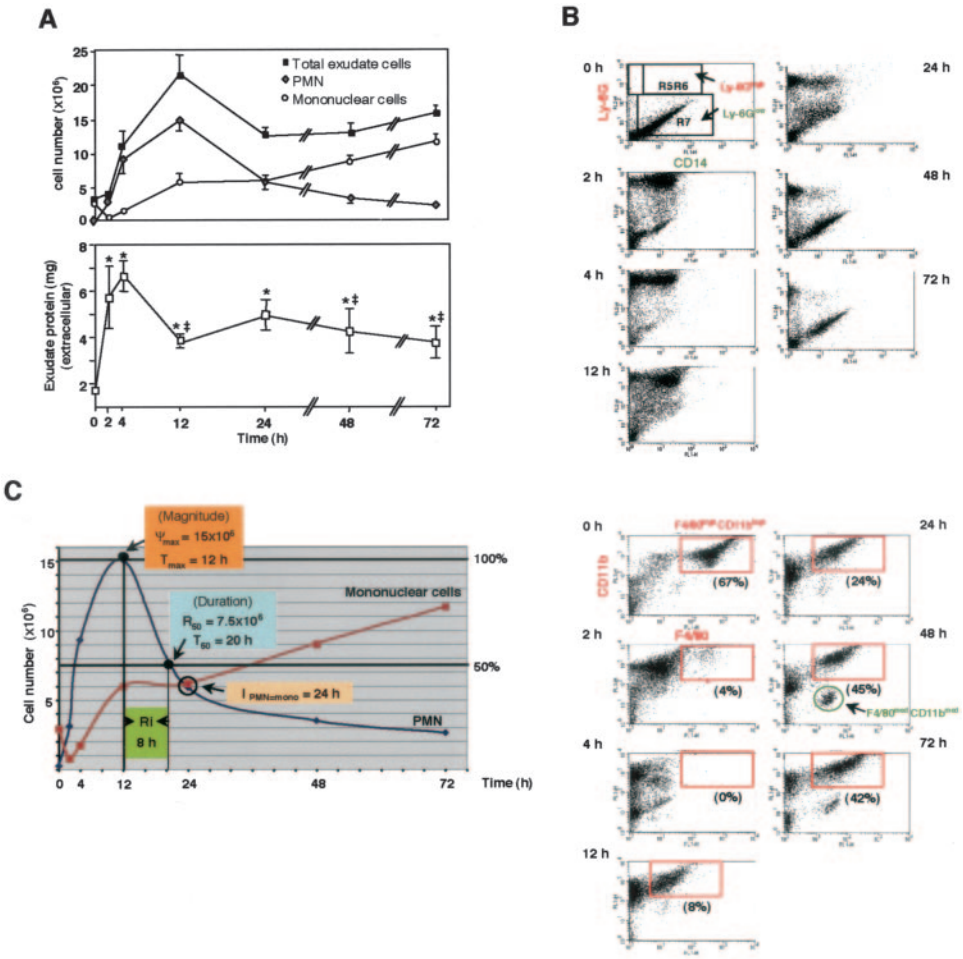

FIGURE 2. Peritoneal leukocyte composition and protein extravasation: resolution indices. *A*, Time course, leukocyte and exudate proteins. Murine peritoneal lavage was collected at indicated time points and total leukocytes were enumerated by light microscopy. PMN and mononuclear cells were determined by differential leukocyte counting and expressed as cell number ($\times 10^6$) obtained from each peritoneal exudate sample. Cell-free lavage fluids were also collected and total extracellular protein levels were determined by the method of Lowry (22) and expressed as total amount (milligrams) in each peritoneal exudate sample. $*$, $p = 0.05$ when compared with time 0 h; ‡, $p = 0.05$ when compared with time 4 h. Data represent mean ± SEM from $n = 7$–21. *B*, FACS analysis. Lavage cells were stained with anti-mouse CD14 and anti-mouse Ly-6G (*upper panel*). Ly-6G^{low} represents mononuclear cells and Ly-6G^{high} represents PMN; or anti-mouse CD11b and anti-mouse F4/80 (*bottom panel*). F4/80^{high}CD11b^{high} (boxed) represents mature macrophages. A distinct cluster characterized by F4/80^{Med}CD11b^{Med} (circled) may represent a subpopulation of macrophage. Results are representative from three experiments. *C*, The resolution of acute inflammation was defined in operative and quantitative terms by the following resolution indices: 1) magnitude (Ψ_{max}, T_{max}), the time point (T_{max}) when PMN numbers reach maximum (Ψ_{max}); 2) duration (R_{50}, T_{50}), the time point (T_{50}) when the PMN numbers reduce to 50% of Ψ_{max} (R_{50}); 3) R_i, the time interval from the maximum PMN point (Ψ_{max}) to the 50% reduction point (R_{50}) (i.e., $T_{50} - T_{max}$); and 4) point of intersection ($I_{PMN=mono}$), the time point when the increase in mononuclear cells intersects the decrease in PMN (i.e., PMN numbers = mononuclear cell numbers).

Associates). For LC-UV-MS-MS analysis, a ThermoFinnigan LCQ liquid chromatography ion trap tandem mass spectrometer was used and equipped with a LUNA C18-2 (100 × 2 mm × 5 μm) column and a rapid spectra scanning UV diode array detector that monitored UV absorbance ~0.1–0.2 min before samples entering the MS-MS (30). A standard mixture of AA, EPA, DHA, 17*S*-hydroxy-docosahexaenoic acid (17*S*-HDHA), and 10,17*S*-DT was used to obtain standard curves for each compound. Linear regression gave R-square values of 0.86–0.99 for each standard curve. Detailed procedures for isolation, quantitation, and structural determination of lipid-derived mediators used in this study were essentially as described (16, 31). Eicosanoid ELISAs were conducted following manufacturer's instructions (PGE_2, leukotriene B_4 (LTB_4), and LXA_4 ELISA from Neogen, and PGD_2-MOX ELISA from Cayman Chemical).

Chemokine/cytokine determinations

Aliquots of supernatants were used to quantitate chemokines and cytokines using a SearchLight Mouse Chemokine Array custom designed with Pierce Boston Technology Center. The SearchLight array uses a special plate prespotted with 16 different capture Abs per well. Following a simple ELISA procedure, the entire plate is imaged to capture chemiluminescent signal generated at each spot within the array. The SearchLight CCD Imaging and Analysis System features image analysis software that calculates concentrations (picograms per milliliter) for unknowns from standard curves.

Statistical analysis

In vitro and in vivo experiments were analyzed by Student's *t* test with p values ≤ 0.05 taken as statistically significant.

Results

Defining the R_i in murine peritonitis

To define the resolution phase and its components, we first determined the cellular changes using a widely used murine peritonitis model (see *Materials and Methods*). A microbial stimulus (zymosan A) was administered i.p. and peritoneal exudates were collected during a 72-h period (Fig. 2*A*). Total leukocyte numbers

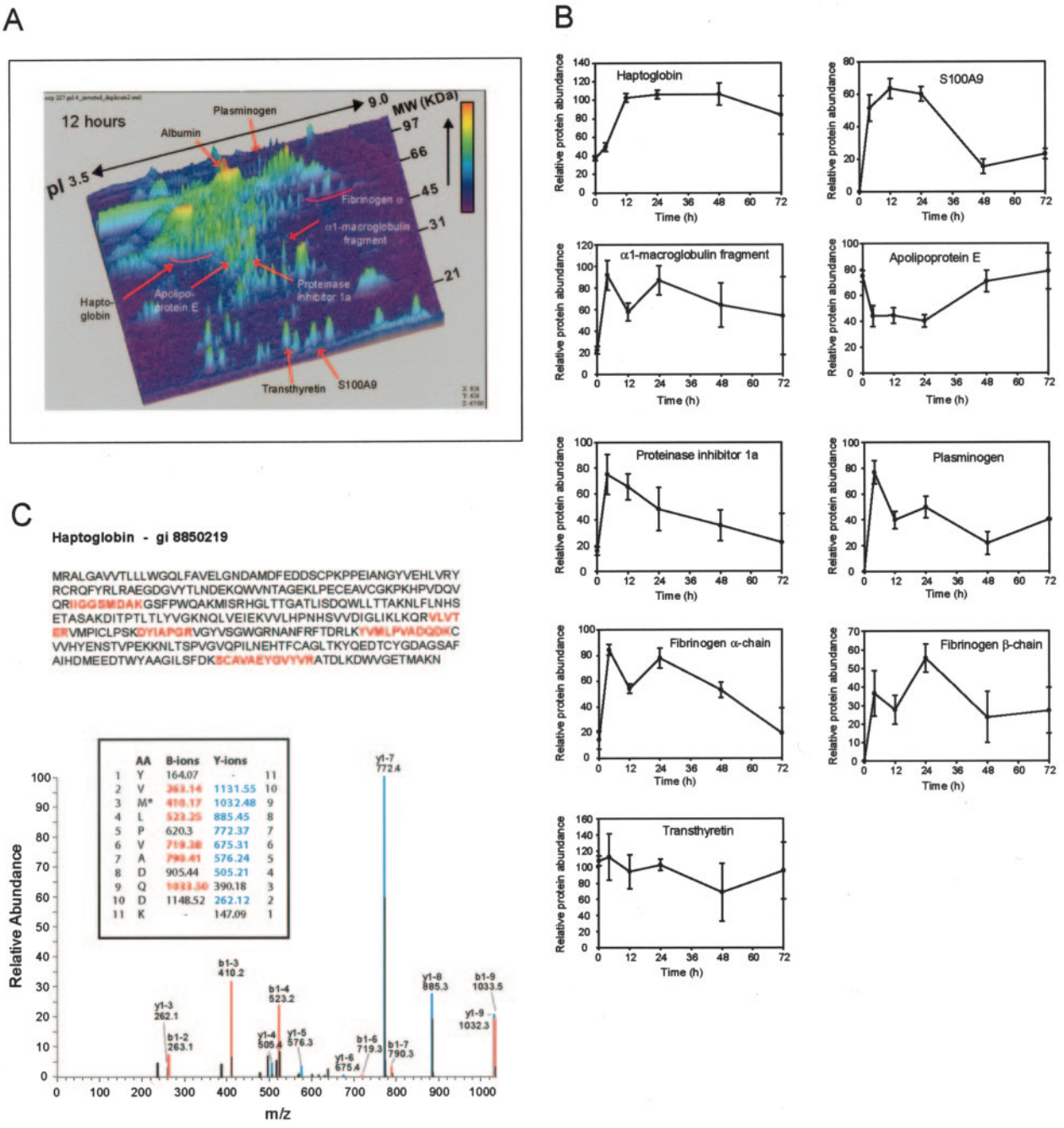

FIGURE 3. Proteomic temporal analysis of exudate proteins. *A*, Mice were injected with zymosan A to induce peritonitis. Exudate fluid was collected at indicated time points and proteins were separated by 2D-gel electrophoresis. Changes in individual protein levels were measured by image analysis. Selected proteins that display temporal regulation are indicated (arrows) and were identified by LC-MS-MS and peptide mapping. *B*, The temporal profiles of several exudate proteins (haptoglobin, S100A9, a C-terminal fragment of α_1-macroglobulin, apolipoprotein E, proteinase inhibitor 1α, plasminogen, the fibrinogen α- and β–chains, and transthyretin) are shown (values are means $\pm$ SEM, $n = 3$–6 gels). *C*, Tryptic peptide mapping of haptoglobin by mass spectrometry. Peptides that are matched are shown in red. The matching of the tandem mass spectrum of peptide YVMLPVADQDK is shown.

increased at 4 h with a maximal infiltration at 12 h ($22 \pm 2 \times 10^6$ cells); this infiltrate was predominantly composed of PMN as determined by the cell surface marker Ly-6G (Fig. 2*B*, *upper panel*). The number of monocytes/macrophages initially dropped at 2 h, then gradually increased until 12 h (Fig. 2*A*). The macrophage population was also determined by double staining with macrophage markers F4/80 and CD11b (Fig. 2*B*, *bottom panel*). The resident macrophage is the predominant mononuclear cell type in naive mice (67% of total cells), which sharply decreased after initiation of inflammation (4% at 2 h and not detected at 4 h). Thus the mononuclear cell population in the early inflammation phase is mainly composed of influxed monocytes (18% at 2 h and 16% at 4 h, Fig. 2*A*). At later time points, macrophage numbers gradually returned so that at 48–72 h they became the major cell type in the peritoneal exudate (42–45%), consistent with their known action in promoting resolution. In this context, it is of interest to note the emergence of a distinct macrophage subpopulation characterized by $F4/80^{med}CD11b^{med}$ that represent 7% and 4% of the total cells at 48 and 72 h, respectively. The phenotype of this subpopulation might represent specialized "proresolving" macrophages.

Table I. *Peritoneal exudate proteins that display temporal changes: identified peptide fragments, m.w., pI, and cross-correlation scores*

Protein	GenInfo Identifier Entry	m.w. Observed	pI Observed	m.w. Predicted	pI Predicted	% Coverage	Identified Peptides	Cross-Correlation
Haptoglobin	8850219	48	5.1	38.7	5.88	23	LRAEGDGVYTLNDEK	3.239
							AEGDGVYTLNDEK	3.112
							DITPTLTLYVGK	2.749
							YVM*LPVADQDK	2.647
							NQLVEIEK	2.204
							SC#AVAEYGVYVR	1.920
							DYIAPGR	1.316
							VLVTER	1.199
							IIGGSMDAK	1.115
							IIGGSM*DAK	1.023
S100A9	6677837	15	6.7	13.1	6.65	23	QMVEAQLATFM*K	2.197
							QM*VEAQLATFM*K	1.966
							SITTIIDTFHQYSR	1.210
$[Alpha]_1$-Macroglobulin (fragment)	6680608	36	6.5	166	6.27	*	EVLVTSRSSGTFSK	3.551
							TEVNTNHVLIYIEK	3.224
							LQDQPNIQR	2.583
							DLSSSDLSTASK	2.527
							YNILPVADGK	2.381
							LLLQEVR	2.224
							M*VSGFIPM*KPSVK	2.022
							LPDLPGNYVTK	1.186
Apolipoprotein E	114041	37	5.6	35.8	5.56	9.3	GRLEEVGNQAR	2.542
							LQAEIFQAR	1.626
							LGPLVEQGR	1.072
Serine (or cysteine) proteinase inhibitor 1α	6678079	36	5.9	46	5.44	7.2	TLM*SPLGITR	1.805
							LSISGEYNLK	1.786
							M*QHLEQTLSK	1.392
Plasminogen	31982113	95	6.3–6.8	90.7	6.21	7.3	GSDVQEISVAK	3.798
							M*RDVILFEK	2.006
							HSIFTPQTNPR	1.953
							LILEPNNR	1.733
							EAQLPVIENK	1.440
							VILGAHEEYIR	1.289
Fibrinogen α-chain	33563252	57–60	6.7–8.2	61.3	7.2–8.0	22.6	AQQIQALQSNVR	4.168
							GLIDEANQDFTNR	3.302
							EINLQDYEGHQK	2.345
							NSLFDFQR	2.320
							M*SPVPDLVPGSFK	2.305
							M*ELERPGK	2.210
							GDKELLIGK	2.024
							NIM*EYLR	1.875
							RIEILR	1.889
							RLEVDIDIK	1.836
							AQLIDM*K	1.157
							ELLPTK	1.012
							QLQQVIAK	1.045
							QYLPALK	0.672
Fibrinogen β-chain	20872398	55	6–6.5	54.7	6.68	14.8	LESDISAQMEYCR	3.243
							AHYGGFTVQNEASK	3.164
							M*GPTELLIEM*EDWK	2.717
							GFGNIATNEDAK	2.664
							SILEDLR	2.184
							IRPFFPQQ	1.911
							YQVSVNK	1.710
							EC#EEIIR	1.228
							QDGSVDFGR	1.193
Transthyretin	7305599	16	6.2	15.7	5.75	44.9	GSPAVDVAVK	4.250
							TSEGSWEPFASGK	2.921
							KTSEGSWEPFASGK	2.267
							GSPAVDVAVKVFK	2.270
							TAESGELHGLTTDEK	1.798
							FVEGVYR	1.744
							CPMLVKVLDAVR	1.352
							VELDTK	1.519
							CPLMVK	1.001
							VLDAVR	0.642

*, The observed protein spot is ~36 kD; all peptide hits are in the C-terminal domain (amino acids 1241–1441) of the full-length protein.

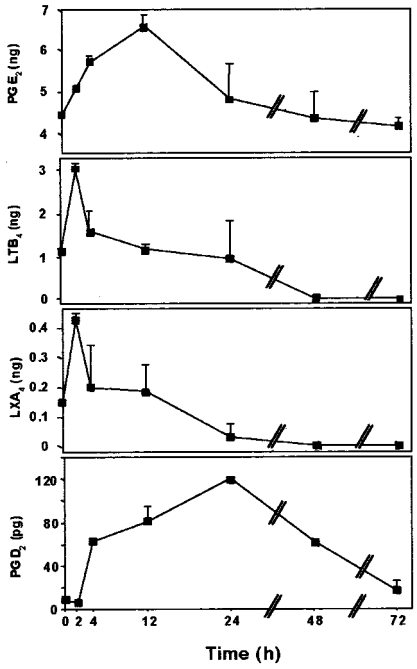

FIGURE 4. Eicosanoid generation during resolution. Cell-free fluids from murine peritoneal lavage were collected at indicated time points. LXA_4, LTB_4, PGE_2, and PGD_2 amounts were determined by ELISA. Data represent mean ± SEM ($n = 3$) and were expressed as amounts detected in each mouse.

These results are consistent with the current working definition of cellular inflammation-resolution (for recent review see Ref. 2), namely that PMN are the first effector leukocytes trafficking into the exudate, followed by mononuclear cells. Therefore, we defined resolution in quantitative terms with these two cell types. Between 12 h (T_{max}) and 20 h (T_{50}), total PMN numbers decreased from 15×10^6 (Ψ_{max}; maximal PMN number) to 7.5×10^6 (R_{50}; essentially 50% reduction of PMN), whereas mononuclear cell numbers apparently did not change within the exudate. For the purpose of direct comparison, we termed this period of neutrophilic loss from the exudate (i.e., 12–20 h) the R_i (Fig. 2*C*). At 24 h, PMN number equals the infiltrated monocyte number in the exudate; we termed this time point the intersection point ($I_{PMN=mono}$). This set of resolution indices provides operative and unbiased assessments of resolution that can be used to evaluate the impact of and/or proresolving properties of endogenous and synthetic anti-inflammatory agents.

Between 24 and 72 h after the initiation (T_0) of inflammation, PMN gradually disappeared, whereas monocytes increased, so that at 72 h, monocytes (Ly-$6G^{low}$) made up ~80% of the exudate cells (Fig. 2, *A* and *B*). Protein levels within exudates followed a dissimilar time course compared with cellular changes; there was a rapid increase in exudate protein amounts that peaked at 4 h (6.7 ± 0.8 mg) and a subsequent significant decrease to ~50% of the peak level at 12 h, after which a minor second phase of protein accumulation was observed (Fig. 2*A*).

Temporal proteomic analysis of exudate proteins: identification of potential "resolvers" as protein activators in resolution circuits

To determine the temporal changes of specific exudate proteins, we used a mass spectrometry-based proteomic analysis with 2D-gel electrophoresis and image analysis. Proteins were identified by peptide mapping of in-gel-digested proteins using capillary liquid chromatography-nanospray ion trap tandem mass spectrometry (nanospray-LC-MS-MS) and bioinformatics software. Fig. 3 shows a representative 2D-gel of exudate proteins and the temporal profiles of several proteins with distinct kinetics during inflammation-resolution. A list of proteins and their corresponding identified tryptic peptide fragments together with cross-correlation scores are included in Table I, as well as the observed and theoretical (m.w.) and isoelectric point (pI) of the identified proteins. Serum proteins such as plasminogen, fibrinogen, and serum albumin were abundant in exudates 4 h after initiation of inflammation, indicating that

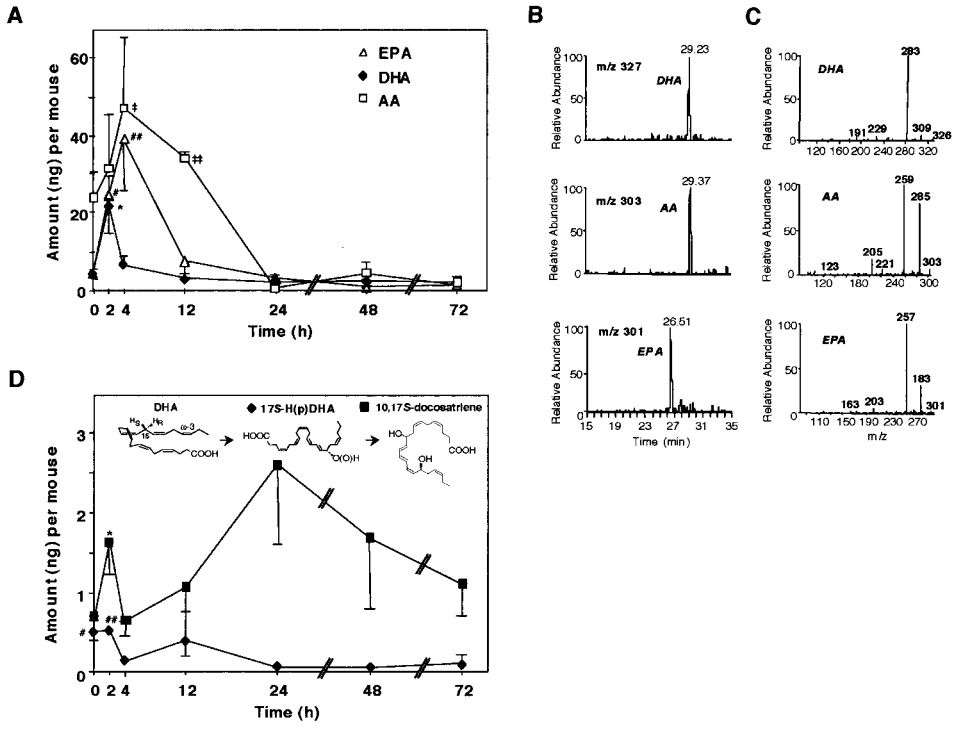

FIGURE 5. Generation of lipid mediators and their precursors. *A*, DHA, EPA, and AA were analyzed and quantitated by LC-UV-MS-MS. For DHA, *, $p = 0.01$ when compared with time 0 and 4 h. For EPA, #, $p = 0.02$ when compared with time 0. ##, $p = 0.01$ and 0.03 when compared with time 0 and 12 h, respectively. For AA, ‡, $p = 0.03$ and ‡‡, $p = 0.01$ when compared with time 24 h. *B*, SIM chromatographs; and *C*, MS-MS spectra of DHA (m/z 327), AA (m/z 303), and EPA (m/z 301) were obtained from lavage collected at 4 h. *D*, DHA-derived products, namely 17-HDHA and 10,17*S*-docosatriene were determined by LC-UV-MS-MS. For 17*S*-HDHA, #, $p = 0.05$ and ##, $p < 0.01$ when compared with time 4 h. For 10,17*S*-docosatriene, *, $p = 0.04$ and 0.02 when compared with time 0 and 4 h, respectively. Data represent mean ± SEM ($n = 3$–5) and were expressed as amounts (nanograms) detected in each mouse (*A* and *D*).

protein exudation from blood made the largest contribution to the total exudate protein levels (Fig. 2*A*). Haptoglobin (Fig. 3, *B* and *C*) displayed a delayed accumulation that is maximal at the onset of R_i. S100A9 rapidly accumulated in the exudate, achieving maximal levels during R_i, followed by a gradual decrease at 24 h. The exudate level of a C-terminal fragment of α_1-macroglobulin (pregnancy zone protein), plasminogen, and fibrinogen displayed the same kinetics as the total exudate protein levels (Fig. 2*A*). In contrast, apolipoprotein E was present in the uninflamed peritoneum; its levels decreased during the R_i and returned to basal levels after 24 h. Proteinase inhibitor 1a rapidly appeared in the peritoneal exudate, with maximal levels at 4 h that thereafter decreased continuously. Transthyretin levels apparently did not change during the time course (Fig. 3*B*). Together, using this approach of "resolution proteomics" we identified several components that are potential founding members of the resolvers in novel resolution circuits and pathways.

Exudate eicosanoids and novel lipid mediators: resolvins and 17S-series docosatrienes and protectins

During inflammation within a confined space such as the peritoneum, marked temporal changes occur in the formation of both proinflammatory and anti-inflammatory eicosanoids (1, 7). In this study, PGE_2, a signal that can activate the full LXA_4-biosynthetic capacity in vivo (7), was present in the peritoneum before peritonitis and elevated during the acute inflammatory response (Fig. 4), mirroring the time course of PMN infiltration. The maximal levels of both LTB_4 and LXA_4 were observed at 2 h and subsequently subsided during the first 24 h (Fig. 4). In comparison, PGD_2 level was low at the initiation of inflammation, then gradually increased during the R_i and peaked at 24 h. These values were monitored by ELISA because they were below the limit of detection via LC-MS-MS (see *Materials and Methods*).

In addition to AA, DHA and EPA are also precursors of recently uncovered bioactive lipid mediators, namely resolvins, docosatrienes, and neuroprotectins (9, 17). In contrast to the well-appreciated proinflammatory eicosanoids derived from AA (32), these novel lipid mediators, together with LXA_4 and ATL, represent the first identified endogenous anti-inflammatory lipid mediators. Therefore, we determined the levels of their precursors AA, EPA, and DHA in the exudates by LC-UV-MS-MS (Fig. 5*A*), and their identities were verified by physical properties including retention times and mass spectra that matched authentic standards (Fig. 5, *B* and *C*). Notably, we found a rapid increase of EPA (38.9 ng/exudate at 4 h, $p \leq 0.01$) and DHA (21.7 ng/exudate at 2 h, $p = 0.01$) (Fig. 5*A*), which returned to essentially basal levels at 12 h. In comparison, AA was present from 0 to 12 h (14.3–47.3 ng/exudate), which markedly decreased during R_i (i.e., 12–24 h) (Fig. 5*A*). Interestingly, the DHA-derived oxygenation product 17*S*-HDHA was present from 0 to 2 h (0.5 ng/exudate) and gradually decreased thereafter (Fig. 5*D*). In comparison, there was a transient appearance of 10,17*S*-docosatriene at 2 h after administration of zymosan A (1.6 ng/exudate, $p = 0.04$), which returned to basal levels at 4 h. In addition, the decrease in 17*S*-HDHA coincided with the second phase appearance of 10,17*S*-docosatriene that gradually increased during R_i and reached maximal levels at 24 h (2.6 ng/exudate), suggesting that this novel omega-3 PUFA-derived mediator plays a role during resolution.

Temporal relationships with chemokines and cytokines

Given the important roles that chemokines and cytokines play in inflammation (4) and that some have been implicated in resolution and anti-inflammation, i.e., IL-10, IL-4, and IL-13, we monitored the temporal changes of a panel of chemokines and cytokines to assess whether any were associated with the R_i and the resolution phase. With the exception of TGF-β and stromal cell-derived factor-1β, the key chemokines/cytokines associated with leukocytes and inflammation displayed maximal exudate levels at 2 or 4 h, after which the levels rapidly decreased before maximal appearance of PMN (i.e., T_{max}) (Fig. 6). In contrast to other cytokines, TGF-β levels gradually increased during the R_i and reached maximal levels of 1.3 ng/mouse at 24 h, suggesting that TGF-β plays a critical role in resolution of acute inflammation.

Resolvins and protectins regulate leukocyte trafficking and cytokine/chemokine production

Because AA-derived LXA_4, EPA-derived RvE1, and DHA-derived 10,17*S*-docosatriene are produced endogenously (Figs. 4 and 5*D*) (7, 9, 16), we sought to examine whether they can regulate cellular composition and molecular components involved in resolution of acute inflammation. To this end, ATLa (a 15-epi-LXA_4 stable analog), a known stop signal for PMN infiltration (14), was directly compared with the actions of RvE1 and 10,17*S*-docosatriene (Fig. 1), each locally administered just before initiation of peritonitis. Each of these compounds reduced total leukocytes and PMN infiltration (Fig. 7), but displayed different kinetics; ATLa's action appeared earliest at 4 h to regulate cellular infiltration, whereas RvE1 and 10,17*S*-docosatriene gave maximal inhibition at 12 h. Both ATLa and 10,17*S*-docosatriene triggered mononuclear cell infiltration at 4 h, and 10,17*S*-docosatriene inhibited mononuclear cell accumulation at 12 h. In parallel determinations by

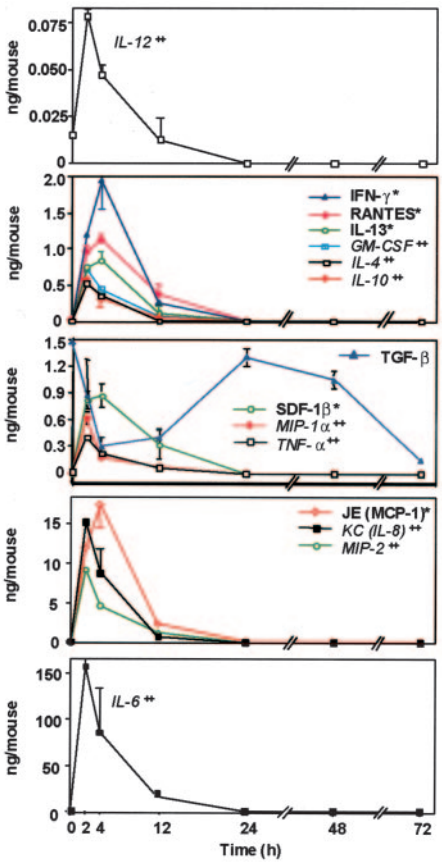

FIGURE 6. Chemokine/cytokine production during resolution. Cell-free fluids from murine peritoneal lavage were collected at indicated time points. Amounts of selected chemokines and cytokines were measured by multiplexed sandwich ELISA. The protein levels that peaked at either 2 h (++) or 4 h (*) are indicated. Results are expressed as total amount (nanograms) per peritoneal exudate sample. Data represent mean ± SEM ($n = 3$).

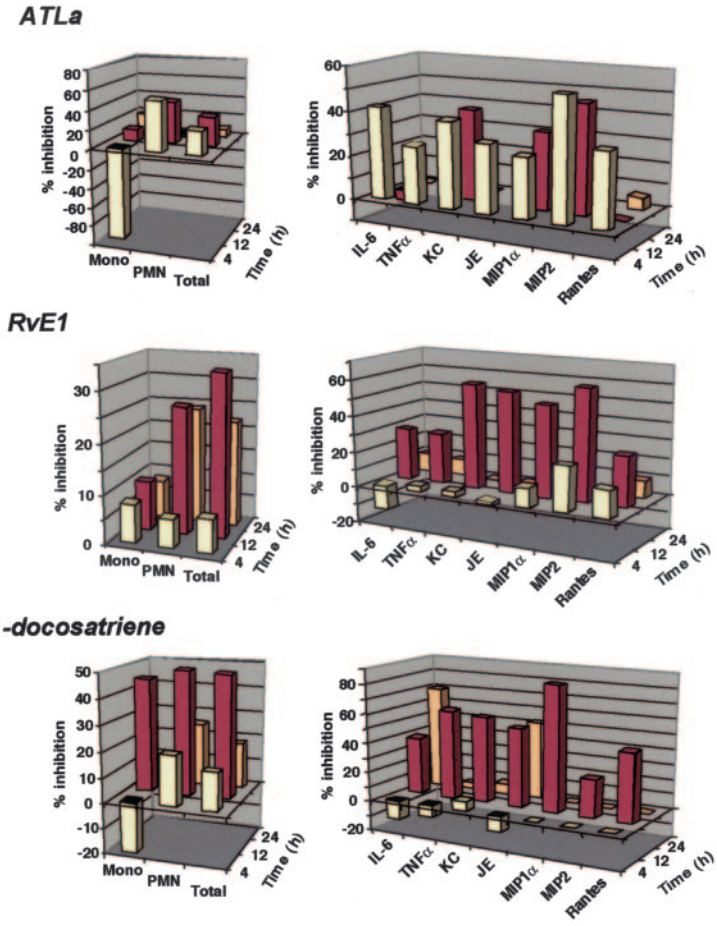

FIGURE 7. Novel lipid mediators regulate leukocyte trafficking and cytokine/chemokine release. Mice were injected with ATLa, RvE1, 10,17*S*-docosatriene (300 ng i.p.), or vehicle alone and followed by i.p. injection of 1 mg of zymosan A. Peritoneal lavages were obtained at indicated time points and leukocytes were enumerated. Cell-free fluids were collected and amounts of selected proinflammatory cytokines and chemokines were determined by multiplexed sandwich ELISA. Results are expressed as percent inhibition compared with mice injected with zymosan A alone. Data represent mean from three independent experiments.

FACS analysis, neither of these compounds changed the percentage of macrophage population at 12 h. When the resolution indices were calculated for these compounds, it was apparent that ATLa lowered Ψ_{max} without changing the duration (R_i) or onset (T_{max}) of resolution in this system (Fig. 8 and Table II). This is in sharp contrast to both RvE1 and 10,17*S*-docosatriene, which initiated R_i at earlier time intervals (T_{max} = 8 and 5 h, respectively); furthermore, 10,17*S*-docosatriene shortened the duration of R_i to 6 h. Total exudate protein levels were not significantly changed by either ATLa, RvE1, or 10,17*S*-docosatriene (data not shown).

Their differential actions were also observed in regulating cytokines/chemokines (Fig. 7); again, ATLa, a known regulator of chemokines (14), markedly inhibited proinflammatory cytokines/chemokines (e.g., IL-6, TNF-β, KC, JE, MIP-1α, MIP-2, and RANTES), which was most striking at 4 h (20–50% inhibition). In comparison, the novel RvE1 and 10,17*S*-docosatriene each gave inhibitory actions that were not evident at 4 h but clearly reached maximum at 12 h (30–80% inhibition). The bioactions of these lipid mediators (i.e., inhibition of PMN infiltration and proinflammatory chemokines/cytokines) coincided with their respective time courses of in vivo generation in that LXA_4 appeared 2–4 h after zymosan A stimulation while 10,17*S*-docosatriene levels peaked at 12 h. Interestingly, ATLa significantly increased exudate TGF-β levels at 4 and 12 h after inflammation (Fig. 9). In the absence of peritonitis, ATLa alone did not stimulate TGF-β (data not shown). Taken together, each of these endogenous anti-inflammatory lipid mediators selectively altered cellular composition, chemokine/cytokine production, and resolution indices.

Discussion

In the present study, we used two unbiased mass spectrometry approaches that permit direct identification of the major lipid mediators and proteins in resolution, namely tandem LC-UV-MS-MS-based lipidomic and proteomic analyses coupled with bioinformatics (Fig. 1). Using this approach, we determined the temporal changes in the cellular and molecular components in a widely studied and standard murine model of a self-resolving inflammation. The initial response is composed of an early phase (0–12 h) characterized by the PMN influx followed by monocyte infiltration and a transient exudation of serum proteins. This early phase also displayed rapid formation (0–4 h) of both LTB_4 and LXA_4 from AA with essentially identical kinetics.

Also we found the presence of DHA, EPA, and AA at local site(s) of inflammation in vivo. We recorded the exudate volume at 2 h after inflammation (0.47 $\pm$ 0.02 ml) and estimated that the exudate levels of unesterified DHA, EPA, and AA were 141, 172, and 218 nM, respectively, and may reflect stimulated release of EPA and DHA from lipid storage sites. The early involvement of $iPLA_2$, a calcium-insensitive phospholipase A_2 that can release DHA (33), in AA release was recently demonstrated in acute pleural inflammation (34). In this respect, we found via proteomic analysis that S100A9, a known AA-binding protein (35), was present in the exudate within 2 h after initiation of inflammation and reached maximal at the onset of R_i, paralleling the PMN infiltration time course (Figs. 2*A* and 3*B*). S100A9 is a cytosolic PMN protein that can be secreted and exhibits potent actions on inflammatory cell recruitment (35). In addition, α_1-

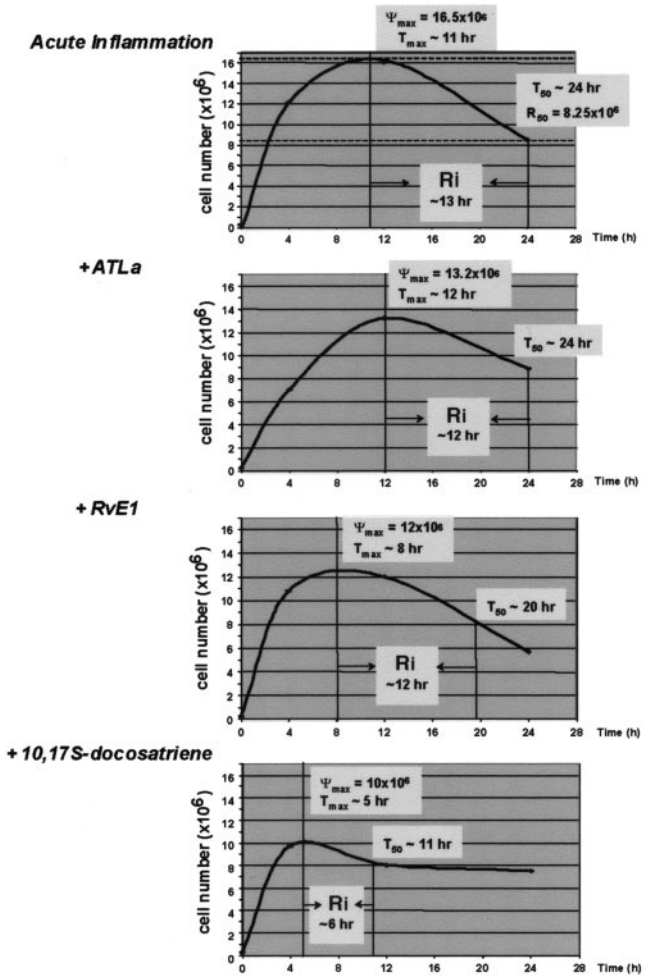

FIGURE 8. Novel lipid mediators specifically change resolution indices. During acute inflammation, PMN infiltration reached maximum ($\Psi_{max} = 16.5 \times 10^6$) at ~11 h ($T_{max}$) and reduced to 50% ($R_{50} = 8.25 \times 10^6$) by ~24 h ($T_{50}$), giving the R_i ~13 h. When ATLa, RvE1 or 10,17*S*-docosatriene was administrated, the T_{50} for each compound was determined as the time point when PMN equals 8.25×10^6 (R_{50}). Each compound differentially altered the resolution indices. For example, 10,17*S*-docosatriene shifted T_{max}, T_{50} and shortened R_i, whereas RvE1 shifted only T_{max} and T_{50}. All three compounds reduced Ψ_{max}. Data are representative from $n = 5$–6.

macroglobulin, similar to α_2-macroglobulin, binds several proteinases including tissue-plasminogen activator and promotes their clearance (36). Thus, it is possible that α_1-macroglobulin, like α_2-macroglobulin, also plays a role in the removal of proinflammatory cytokines in the exudate and/or lowering these effective local concentrations before the onset of resolution (37).

Because resolution is currently defined only by visual inspection at the level of light microscopy, i.e., the histological appearance of an inflamed tissue, we introduce in this study a set of resolution indices to define R_i as the time interval from the recorder maximum PMN infiltration point to the 50% reduction point. In addition to loss of PMN, this interval (12–20 h) was marked by distinct molecular events: 1) haptoglobin levels peaked at the onset of R_i; haptoglobin is an acute-phase protein that has microbicidal activity and, by binding to hemoglobin, confers protection from oxidative damage (38), and activates CD163, a scavenger receptor that triggers anti-inflammatory and atheroprotective pathways (39); 2) a second phase of increase in exudate 10,17*S*-docosatriene was observed during R_i; note that DHA (16) is rapidly converted to 17*S*-HDHA (Fig. 5*D*, *inset*); 3) TGF-β levels rise markedly during the R_i; this cytokine is released by macrophages during the nonphlogistic removal of the apoptotic PMN (40); and 4) PGE_2 reached maximal levels at the onset of resolution and declined during R_i; the decrease of PGE_2 coincided with the increase of PGD_2 levels, which peaked at 24 h.

Differential regulation of PGE_2 and PGD_2 formation in murine macrophages has been described earlier, in that proinflammatory cytokines increase PGE_2 and decrease PGD_2 synthesis (41). PGE_2 is commonly considered as a proinflammatory mediator. In contrast, it displays beneficial actions in the lung in limiting inflammatory response and promoting tissue repair (2, 34, 42). Also, PGE_2 is a potent anti-inflammatory and immunoregulatory agent in allergic airway responses (43). Along these lines, recent findings demonstrated that both PGE_2 and/or PGD_2 switch eicosanoid biosynthesis from predominantly "proinflammatory" LTB_4 to "anti-inflammatory" LXA_4 production that stops PMN infiltration in the murine air pouch (7). In comparison, our present results showed the rapid formation of LTB_4 and LXA_4 (i.e., 2–4 h), followed by late appearance of PGE_2 (i.e., 12 h). This is a different temporal pattern than that observed in TNF-α-stimulated acute inflammation in the murine air pouch, a de facto wound model, where PMN acquire the capacity to biosynthesize LXA_4 during the later stages of inflammation, and class-switching of eicosanoids from PGE_2 to LXA_4 initiates resolution. The different kinetics in eicosanoid generation might likely reflect the nature of the experimental models (microbial-initiated vs wound model) and/or the stimulus-specific signaling pathways (zymosan A vs TNF-α). Thus, in zymosan A-initiated acute inflammation, it is likely that both PGE_2 and PGD_2 play a role in promoting resolution. Taken together, these results indicate that functionally distinct lipid mediator profiles switch during acute exudate formation to "reprogram" the exudate PMN to promote resolution.

At the post-R_i catabasis period (20 h), mononuclear cells/macrophages become the dominant cell type in the peritoneum. Total exudate protein levels decreased and specific proteins that originated from serum disappeared, whereas proteins that were locally formed, such as apolipoprotein E, returned to normal levels. In

Table II. *Change of resolution indices by novel lipid mediators*

	Ψ_{max} (PMN No. ($\times 10^6$))	T_{max} (h)	T_{50} (h)	R_i (h)
Acute inflammation	16.0 ± 0.7	12.0	26.4 ± 0.9	14.4 ± 0.9
+ ATLa	**11.7 ± 1.3***	12.0	26.0 ± 0.8	14.0 ± 0.8
+ RvE1	**11.6 ± 0.8****	**9.3 ± 0.7****	**21.0 ± 0.6****	11.7 ± 0.3
+ 10, 17*S*-docosatriene	**9.3 ± 0.5****	**4.0****	**11.3 ± 0.7****	**7.3 ± 0.7****

Data represent mean ± SEM ($n = 5$–6) and were analyzed by Student's two-tailed *t*-test.

* $p = 0.03$, ** $p < 0.01$. All three compounds significantly reduced Ψ_{max} (maximal PMN numbers). In addition, RvE1 shifted T_{max} and T_{50} to earlier time points with no significant change of R_i. Furthermore, 10,17*S*-docosatriene significantly altered T_{max} and T_{50} as well as shortened R_i.

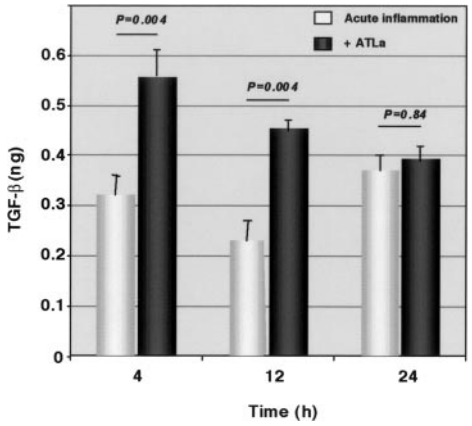

FIGURE 9. ATLa evokes TGF-β release. TGF-β amounts in the cell-free lavage fluids obtained from peritonitis alone or with ATLa were determined by ELISA. Data represent means from duplicates of $n = 3$ and were expressed as amounts (nanograms) in each mouse.

addition, lipid mediators and their precursors returned to basal levels.

Next, it was of interest to determine whether novel lipid mediators alter specific resolution indices, namely, if resolution can be activated or accelerated. Using a differential temporal analysis we found that ATLa, RvE1, and 10,17*S*-docosatriene each modulated resolution with distinct profiles (Figs. 7 and 8). ATLa inhibits specific characteristics of the early proinflammatory phase (PMN infiltration and proinflammatory cytokines/chemokines release) and enhanced TGF-β at 4 and 12 h. Given the known impact of TGF-β in tissue repair and wound healing (44), the appearance of TGF-β is likely to reflect ATLa's stimulatory action on nonphlogistic phagocytosis of apoptotic PMN (45). Hence, lipoxin-stimulated TGF-β formation is likely to be part of a lipoxin-activated resolution circuit. In comparison, administration of RvE1 and 10,17*S*-docosatriene activated and shifted resolution to earlier time points (Fig. 8). 10,17*S*-docosatriene furthermore shortened the R_i, suggesting its impact on accelerating resolution.

In summary, we have determined the main molecular features underlying the resolution of acute inflammation and provide a definition of resolution indices. Using side-by-side or parallel lipidomic- and proteomic-based analyses, we identified specific anti-inflammatory and proresolving circuits that are switched on during the resolution. In addition, administration of novel lipid mediators (i.e., ATLa, RvE1, or 10,17*S*-docosatriene) significantly altered resolution indices and regulated specific molecular components. For example, we showed that ATLa reduces Ψ_{max}, the maximal number of neutrophils in the exudate, and RvE1 reduces Ψ_{max} as well as T_{max}, indicating that resolution is initiated at an earlier time. 10,17*S*-docosatriene furthermore shortens and shifts R_i to earlier time points, demonstrating its capacity to activate and accelerate resolution. Thus, our results demonstrated that the resolution of acute inflammation is a dynamic process and that specific molecular circuits/pathways can be activated by small endogenous molecules to promote resolution. Taken together, these findings provide measurable indices for resolution and a molecular basis for potential novel therapeutic interventions where sustained inflammation is a component of the diseases.

Acknowledgments

We thank Tamara Baer, Anthony Lee, and Gabrielle Fredman for excellent technical assistance. Mary H. Small is acknowledged for assistance in the preparation of this manuscript.

Disclosures

The authors have no financial conflict of interest.

References

1. Majno, G., and I. Joris. 1996. *Cells, Tissues, and Disease. Principles of General Pathology.* Blackwell Science, Cambridge.
2. Gilroy, D. W., T. Lawrence, M. Perretti, and A. G. Rossi. 2004. Inflammatory resolution: new opportunities for drug discovery. *Nat. Rev. 3:401.*
3. Gallin, J. L., and R. Snyderman. 1999. *Inflammation. Basic Principles and Clinical Correlates.* Lippincott Williams & Wilkins, Philadelphia.
4. Nathan, C. 2002. Points of control in inflammation. *Nature 420:846.*
5. Godson, C., and H. R. Brady. 2000. Lipoxins: novel anti-inflammatory therapeutics? *Curr. Opin. Investig. Drugs. 1:380.*
6. Perretti, M., and R. J. Flower. 1994. Cytokines, glucocorticoids and lipocortins in the control of neutrophil migration. *Pharmacol. Res. 30:53.*
7. Levy, B. D., C. B. Clish, B. Schmidt, K. Gronert, and C. N. Serhan. 2001. Lipid mediator class switching during acute inflammation: signals in resolution. *Nat. Immunol. 2:612.*
8. Serhan, C. N. 1994. Lipoxin biosynthesis and its impact in inflammatory and vascular events. *Biochim. Biophys. Acta 1212:1.*
9. Serhan, C. N., C. B. Clish, J. Brannon, S. P. Colgan, N. Chiang, and K. Gronert. 2000. Novel functional sets of lipid-derived mediators with antiinflammatory actions generated from omega-3 fatty acids via cyclooxygenase 2-nonsteroidal antiinflammatory drugs and transcellular processing. *J. Exp. Med. 192:1197.*
10. Lawrence, T., D. A. Willoughby, and D. W. Gilroy. 2002. Anti-inflammatory lipid mediators and insights into the resolution of inflammation. *Nat. Immunol. 2:787.*
11. Heasman, S. J., K. M. Giles, C. Ward, A. G. Rossi, C. Haslett, and I. Dransfield. 2003. Glucocorticoid-mediated regulation of granulocyte apoptosis and macrophage phagocytosis of apoptotic cells: implications for the resolution of inflammation. *J. Endocrinol. 178:29.*
12. Clària, J., and C. N. Serhan. 1995. Aspirin triggers previously undescribed bioactive eicosanoids by human endothelial cell-leukocyte interactions. *Proc. Natl. Acad. Sci. USA 92:9475.*
13. Devchand, P. R., M. Arita, S. Hong, G. L. Bannenberg, R.-L. Moussignac, K. Gronert, and C. N. Serhan. 2003. Human ALX receptor regulates neutrophil recruitment in transgenic mice: roles in inflammation and host-defense. *FASEB J. 17:652.*
14. Serhan, C. N., and N. Chiang. 2004. Novel endogenous small molecules as the checkpoint controllers in inflammation and resolution: entree for resoleomics. *Rheum. Dis. Clin. N. Am. 30:69.*
15. Serhan, C. N. 2001. Lipoxins and aspirin-triggered 15-epi-lipoxins are endogenous components of antiinflammation: emergence of the counterregulatory side. *Arch. Immunol. Ther. Exp. 49:177.*
16. Hong, S., L. Gronert, P. R. Devchand, R.-L. Moussignac, and C. N. Serhan. 2003. Novel docosatrienes and 17S-resolvins generated from docosahexaenoic acid in murine brain, human blood, and glial cells. *J. Biol. Chem. 278:14677.*
17. Marcheselli, V. L., S. Hong, W. J. Lukiw, X. H. Tian, K. Gronert, A. Musto, M. Hardy, J. M. Gimenez, N. Chiang, and C. N. Serhan. 2003. Novel docosanoids inhibit brain ischemia-reperfusion-mediated leukocyte infiltration and pro-inflammatory gene expression. *J. Biol. Chem. 278:43807.*
18. Getting, S. J., R. J. Flower, and M. Perretti. 1997. Inhibition of neutrophil and monocyte recruitment by endogenous and exogenous lipocortin 1. *Br. J. Pharmacol. 120:1075.*
19. Kolaczkowska, E., S. Shahzidi, R. Seljelid, N. van Rooijen, and B. Plytycz. 2002. Early vascular permeability in murine experimental peritonitis is comediated by residential peritoneal macrophages and mast cells: crucial involvement of macrophage-derived cysteinyl-leukotrienes. *Inflammation 26:61.*
20. Chiang, N., T. Takano, C. B. Clish, N. A. Petasis, H. H. Tai, and C. N. Serhan. 1998. Aspirin-triggered 15-epi-lipoxin A_4 (ATL) generation by human leukocytes and murine peritonitis exudates: development of a specific 15-epi-LXA_4 ELISA. *J. Pharmacol. Exp. Ther. 287:779.*
21. Ariel, A., N. Chiang, M. Arita, N. A. Petasis, and C. N. Serhan. 2003. Aspirin-triggered lipoxin A_4 and B_4 analogs block extracellular signal-related kinase-dependent TNF-α secretion from human T-cells. *J. Immunol. 170:6266.*
22. Lowry, O. H., N. J. Roseborough, A. L. Farr, and R. J. Randall. 1951. Protein measurement with Folin phenol reagent. *J. Biol. Chem. 193:265.*
23. Wessel, D., and U. I. Flugge. 1984. A method for the quantitative recovery of protein in dilute solution in the presence of detergents and lipids. *Anal. Biochem. 138:141.*
24. Görg, A., W. Postel, and S. Günther. 1988. The current state of two-dimensional electrophoresis with immobilized pH gradients. *Electrophoresis 9:531.*
25. Rabilloud, T., J.-M. Strub, S. Luche, A. van Dorsselaer, and J. Lunardi. 2001. A comparison between Sypro Ruby and ruthenium II tris (bathophenanthroline disulfonate) as fluorescent stains for protein detection in gels. *Proteomics 1:699.*
26. Rosenfeld, J., J. Capdevielle, J. C. Guillemot, and P. Ferrara. 1992. In-gel digestion of proteins for internal sequence analysis after one- or two-dimensional gel electrophoresis. *Anal. Biochem. 203:173.*
27. Mann, M., R. C. Hendrickson, and A. Pandet. 2001. Analysis of proteins and proteomes by mass spectrometry. *Annu. Rev. Biochem. 70:437.*
28. Yates, J. R., III. 1998. Mass spectrometry and the age of the proteome. *J. Mass Spectrom. 33:1.*
29. Eng, J. K., A. L. McCormack, and J. R. Yates, III. 1994. An approach to correlate tandem mass spectral data of peptides with amino acid sequences in a protein database. *J. Am. Soc. Mass Spectrom. 5:976.*

30. Clish, C. B., B. D. Levy, N. Chiang, H. H. Tai, and C. N. Serhan. 2000. Oxidoreductases in lipoxin A_4 metabolic inactivation: a novel role for 15-oxoprostaglandin 13-reductase/leukotriene B_4 12-hydroxydehydrogenase in inflammation. *J. Biol. Chem. 275:25372*.
31. Gronert, K., C. B. Clish, M. Romano, and C. N. Serhan. 1999. Transcellular regulation of eicosanoid biosynthesis. *Methods Mol. Biol. 120:119*.
32. Samuelsson, B. 1991. Arachidonic acid metabolism: role in inflammation. *Z. Rheumatol. 50:3*.
33. Birbes, H., J. F. Pageaux, J. M. Fayard, M. Lagarde, and C. Laugier. 1998. Protein kinase C inhibitors stimulate arachidonic and docosahexaenoic acids release from uterine stromal cells through a Ca^{2+}-independent pathway. *FEBS Lett. 432:219*.
34. Gilroy, D. W., J. Newson, P. Sawmynaden, D. A. Willoughby, and J. D. Croxtall. 2004. A novel role for phospholipase A_2 isoforms in the checkpoint control of acute inflammation. *FASEB J. 18:489*.
35. Nacken, W., J. Roth, C. Sorg, and C. Kerkhoff. 2003. S100A9/S100A8: myeloid representatives of the S100 protein family as prominent players in innate immunity. *Microscop. Res. Tech. 60:569*.
36. Sanchez, M. C., G. A. Chiabrando, H. A. Guglielmone, G. R. Bonacci, G. A. Rabinovich, and M. A. Vides. 1998. Interaction of human tissue plasminogen activator (t-PA) with pregnancy zone protein: a comparative study with t-PA-α_2-macroglobulin interaction. *J. Biochem. 124:274*.
37. LaMarre, J., G. K. Wollenberg, S. L. Gonias, and M. A. Hayes. 1991. Cytokine binding and clearance properties of proteinase-activated α_2-macroglobulins. *Lab. Invest. 65:3*.
38. Wassell, J. 2000. Haptoglobin: function and polymorphism. *Clin. Lab. 46:547*.
39. Philippidis, P., J. C. Mason, B. J. Evans, I. Nadra, K. M. Taylor, D. O. Haskard, and R. C. Landis. 2004. Hemoglobin scavenger receptor CD163 mediates interleukin-10 release and heme oxygenase-1 synthesis: antiinflammatory monocyte-macrophage responses in vitro, in resolving skin blisters in vivo, and after cardiopulmonary bypass surgery. *Circ. Res. 94:119*.
40. Huynh, M. L., V. A. Fadok, and P. M. Henson. 2002. Phosphatidylserine-dependent ingestion of apoptotic cells promotes TGF-β1 secretion and the resolution of inflammation. *J. Clin. Invest. 109:41*.
41. Fournier, T., V. Fadok, and P. M. Henson. 1997. Tumor necrosis factor-α inversely regulates prostaglandin D_2 and prostaglandin E_2 production in murine macrophages: synergistic action of cyclic AMP on cyclooxygenase-2 expression and prostaglandin E_2 synthesis. *J. Biol. Chem. 272:31065*.
42. Vancheri, C., C. Mastruzzo, M. A. Sortino, and N. Crimi. 2004. The lung as a privileged site for the beneficial actions of PGE_2. *Trends Immunol. 25:40*.
43. Martin, J. G., M. Suzuki, K. Maghni, R. Pantano, D. Ramos-Barbon, D. Ihaku, F. Nantel, D. Denis, Q. Hamid, and W. Powell. 2002. The immunomodulatory actions of prostaglandin E_2 on allergic airway responses in the rat. *J. Immunol. 169:3963*.
44. Wahl, S. M. 1999. TGF-β in the evolution and resolution of inflammatory and immune processes: introduction. *Microbes Infect. 1:1247*.
45. Godson, C., S. Mitchell, K. Harvey, N. A. Petasis, N. Hogg, and H. R. Brady. 2000. Cutting edge: lipoxins rapidly stimulate nonphlogistic phagocytosis of apoptotic neutrophils by monocyte-derived macrophages. *J. Immunol. 164:1663*.